Caenorhabditis elegans Genes Required for the Engulfment of Apoptotic Corpses Function in the Cytotoxic Cell Deaths Induced by Mutations in *lin-24* and *lin-33*

Brendan D. Galvin, Saechin Kim[1] and H. Robert Horvitz[2]

Department of Biology, Howard Hughes Medical Institute, Massachusetts Institute of Technology, Cambridge, Massachusetts 02139

ABSTRACT

Two types of cell death have been studied extensively in *Caenorhabditis elegans*, programmed cell death and necrosis. We describe a novel type of cell death that occurs in animals containing mutations in either of two genes, *lin-24* and *lin-33*. Gain-of-function mutations in *lin-24* and *lin-33* cause the inappropriate deaths of many of the P*n*.p hypodermal blast cells and prevent the surviving P*n*.p cells from expressing their normal developmental fates. The abnormal P*n*.p cells in *lin-24* and *lin-33* mutant animals are morphologically distinct from the dying cells characteristic of *C. elegans* programmed cell deaths and necrotic cell deaths. *lin-24* encodes a protein with homology to bacterial toxins. *lin-33* encodes a novel protein. The cytotoxicity caused by mutation of either gene requires the function of the other. An evolutionarily conserved set of genes required for the efficient engulfment and removal of both apoptotic and necrotic cell corpses is required for the full cell-killing effect of mutant *lin-24* and *lin-33* genes, suggesting that engulfment promotes these cytotoxic cell deaths.

D̲URING the development of the *Caenorhabditis elegans* hermaphrodite, 131 of the 1090 somatic cells generated are eliminated by the process of programmed cell death, also called apoptosis (SULSTON and HORVITZ 1977; KIMBLE and HIRSH 1979; SULSTON *et al.* 1983). The identification of the *C. elegans* genes that function in the pathway for programmed cell death has provided valuable insights into this evolutionarily conserved process. For example, molecular identification of the caspase gene *ced-3* defined the first biochemical mechanism of apoptosis (YUAN *et al.* 1993). Caspases are aspartate-specific cysteine proteases that act in apoptosis in all animals (DEGTEREV *et al.* 2003). Similarly, studies of *C. elegans ced-9* (HENGARTNER *et al.* 1992; HENGARTNER and HORVITZ 1994; SHAHAM and HORVITZ 1996) helped establish the function and pathway of action of its human homolog Bcl-2 and of the misregulation of apoptosis as a cause of human cancer (VAUX *et al.* 1988; HOCKENBERY *et al.* 1990; VAUX *et al.* 1992). At least 30 *C. elegans* genes that function in programmed cell death have been identified; many have homologs that function in mammalian apoptosis (HORVITZ 1999; LETTRE and HENGARTNER 2006).

Cells can die not only by apoptosis but also by autophagy and necrosis. In autophagy, cells consume themselves from within, for example, under situations of nutritional deprivation (EDINGER and THOMPSON 2004). There are no known examples of autophagic deaths in *C. elegans*. Necrosis is a cellular death process defined largely by ultrastructure, such as the swelling of organelles and the loss of plasma membrane integrity (ZONG and THOMPSON 2006). Necrosis can be caused by injury or physiological insult and contributes significantly to human disease. Some cell deaths that occur in *C. elegans* are considered to be necrotic (HALL *et al.* 1997). The best understood necrotic deaths in *C. elegans* are those caused by gain-of-function (gf) mutations that alter the mechanosensory sodium channel subunit MEC-4 (DRISCOLL and CHALFIE 1991). The deaths caused by *mec-4(gf)* mutations and by mutations in several other genes, including *deg-1* (which encodes a related channel subunit) (CHALFIE and WOLINSKY 1990), *deg-3* (which encodes an acetylcholine-gated ion channel) (TREININ and CHALFIE 1995), and activated transgenic Gα$_s$ (KORSWAGEN *et al.* 1997; BERGER *et al.* 1998) probably involve similar mechanisms. The *mec-4(gf)* mutations cause the hyperactivation of *deg*enerin/*e*pithelial *Na*$^+$ *c*hannel (DEG/EnaC) channels and cause the deaths of the six touch-receptor neurons that express the MEC-4 subunit (LAI *et al.* 1996). These deaths seem to require release of calcium from the endoplasmic reticulum (XU *et al.* 2001) and the activation of the calcium-activated calpain proteases and of

specific cathepsin aspartyl proteases (Syntichaki *et al.* 2002). This death process is similar to that proposed for mammalian excitotoxic cell death (Driscoll and Gerstbrein 2003).

Here we describe a third type of cell death in *C. elegans.* We refer to this type as cytotoxic cell death. Cytotoxic cell death is distinguishable from programmed cell death and from necrotic cell death on the basis of morphological, genetic, and electron microscopic criteria. We observed the cytotoxic cell deaths of the *C. elegans* P*n*.p hypodermal blast cells in animals containing gain-of-function mutations in either of two genes, *lin-24* or *lin-33*. *lin-24* and *lin-33* appear to act together in causing the cytotoxicity that affects the fates and survival of the P*n*.p cells.

MATERIALS AND METHODS

Strains and general techniques: Strains were cultured as described by Brenner (1974) and grown at 20°. The Bristol strain N2 was used as the wild-type strain, except in multifactor mapping experiments that used the polymorphic wild-type strains N62 (Bergerac) or CB4856 (Williams *et al.* 1992; Wicks *et al.* 2001). The mutations used in the study are listed below and are described, unless otherwise noted, by Riddle *et al.* (1997):

LGI: *ced-1(e1735)* and *ced-12(n3261)* (Zhou *et al.* 2001).
LGIII: *ced-9(n1950)*, *ced-4(n1162)*, *ced-6(n1813)*, and *ced-7 (n1996)*.
LGIV: *lin-24(n432, n1057), lin-24(n1821, n2050)* (S. G. Clark and H. R. Horvitz, unpublished results), *lin-24(n2258, n2333, n4294Δ, n432 n1503)* (this study), *lin-33(n1043, n1044), lin-33(n1110)* (M. K. Edwards and H. R. Horvitz, unpublished results), *lin-33(n1302)* (J. H. Thomas and H. R. Horvitz, unpublished results), *lin-24(n1968, n2003, n4514Δ, n1043 n1502)* (this study), *ced-3(n717), ced-2(e1752), ced-5 (n1812), ced-10(n1993), dpy-4(e1166), dpy-26(n199), unc-22(s7), unc-30(e191), unc-31(e169), unc-44(e362)*, and *lntl-1(n4763Δ)* (this study).
LGV: *unc-76(e911)* and *egl-1(n1084 n3082)* (Conradt and Horvitz 1998).

In addition, we used strains containing the following chromosomal aberrations: *sDf21* (Clark and Baillie 1992), *nDf41* (S. Kim and H. R. Horvitz, unpublished results), and *yDp1* (Delong *et al.* 1987).

lin-24(n2258) was found in the strain CB362 *unc-44(e362)* and was originally identified during the mapping of *lin-33*. Briefly, we had constructed an *unc-5(e53) unc-44(e362)* IV strain with *unc-44(e362)* from strain CB362. We crossed *lin-33(n1043)* males with *unc-5(e53) unc-44(e362)* hermaphrodites and observed that the *lin-33(n1043)/unc-5(e53) unc-44(e362)* cross progeny hermaphrodites did not have a vulvaless phenotype. Given that *lin-33(n1043)/+* hermaphrodites are 77% vulvaless, we postulated that, in the *unc-5(e53) unc-44(e362)* strain, there was also a loss-of-function *lin-33* or *lin-24* allele that suppressed the *lin-33(n1043)/+* vulvaless phenotype. Additional experiments confirmed that our *unc-5(e53) unc-44(e362)* strain as well as CB362 *unc-44(e362)* were homozygous for a *lin-24* allele, which we named *n2258*.

Assay for vulvaless animals: All animals scored had been propagated through at least two generations without starvation. Five-centimeter petri plates were seeded 12–24 hr prior to the assay with 10 μl of an overnight culture of the *Escherichia coli* strain OP50 grown in B broth. Fourth-stage larval (L4) animals were placed singly on petri plates. After 18 hr, plates were examined for the presence of gravid adults. Only petri plates with gravid adults were scored for the presence or absence of eggs; animals on petri plates without any eggs were scored as vulvaless (Vul).

Percentage of suppression was calculated by dividing the penetrance of the vulvaless phenotype of *lin(gf); ced* strains by the penetrance of the vulvaless phenotype of the *lin(gf)* strain, subtracting that number from one and multiplying the result by 100.

To assay for the suppression of heterozygous *lin-24(n432)-* and *lin-33(n1043)*-induced death by loss-of-function alleles of genes that function in programmed cell death, males homozygous for both the *lin(gf)* mutation and the candidate suppressor [*e.g.*, *ced-5(n1812) lin-24(n432)*] were generated by heat shock and mated with strains homozygous for the candidate suppressor and marked with *unc-76(e911)* [*e.g.*, *ced-5(1812); unc-76(e911)*]; 3–5 days later cross-progeny (non-Unc) L4 hermaphrodites were recovered and assayed as described above.

The Vul assays for the dosage studies of *lin-24(n1057)* were performed as previously described (Ferguson and Horvitz 1985). To generate animals of the genotype *lin-24(n1057)/ lin-24(+); yDp1*, we crossed *lin-24(n1057) unc-31(e169)/ lin-24(+) unc-31(+)* males with *dpy-26(n199) unc-31(e169); yDp1* hermaphrodites and picked the hermaphrodite progeny. We determined the Vul phenotype of each animal and by examining its progeny determined the genotype of each animal. Non-Dpy non-Unc animals that segregated Dpy Unc and Lin Unc animals had the genotype *lin-24(n1057) unc-31(e169)/ dpy-26(n199) unc-31(e169); yDp1*. To generate animals with the genotype *lin-24(n1057); yDp1* for analysis, we picked non-Dpy non-Unc progeny of *lin-24(n1057) unc-31(e169)/ dpy-26(n199) unc-31(e169); yDp1* animals. We determined which animals did not segregate Dpy Unc animals and assayed the non-Unc animals.

We used *mDp4* in our attempted dosage studies for *lin-33(n1043)* but very frequent recombination between the free duplication and the chromosomal region under investigation precluded the isolation of strains with the genotypes required for this experiment.

Nomarski observation of P*n*.p cells: P*n*.p cells in *lin-24* or *lin-33* mutant animals were observed using Nomarski differential interference contrast (DIC) microscopy at different times during development as previously described (Sulston and Horvitz 1977).

Electron microscopy: Nomarski DIC microscopy was used to select a nematode with refractile P*n*.p cells, and digital images were taken to note their positions. Mutant animals were recovered from the slide and fixed as previously described (Bargmann *et al.* 1993). The fixed, embedded animals were sectioned as previously described (Gumienny *et al.* 1999) and photographed using a JEOL 12000CX electron microscope at 80 kV. After finding the location of the anus or the gonad in the micrographs, nuclei were counted by examining micrographs of adjacent sections and the images corresponding to the P*n*.p cell that had been identified as abnormal using Nomarski microscopy were examined.

Dominant suppression screen for revertant alleles of *lin-24(n432)* and *lin-33(n1043)*: We mutagenized L4 or early adult hermaphrodites homozygous for either *lin-24(n432)* or *lin-33(n1043)* using ethyl methanesulfonate (EMS) as previously described (Brenner 1974). After mutagenesis, three to four P$_0$ hermaphrodites were placed on individual 5-cm petri plates. F$_1$ self-progeny that were non-Vul were placed singly on petri plates. If >10% of F$_2$ animals on a petri plate were non-Vul, individual non-Vul F$_2$ animals were picked singly to petri plates

and the next generation was assayed for suppression of the Vul phenotype by quantifying the penetrance of the egg-laying defect.

Cloning of *lin-24* and *lin-33*: Using standard three-point and polymorphism mapping, we localized *lin-24(n1057)* and *lin-33(n1043)* to ~300-kb and 156-kb intervals, respectively. To clone the gene *lin-24* we prepared cosmids T20H7, B0001, ZC197, and F20B10 found in the region containing *lin-24* and tested these cosmids (10–50 μg/ml) for ability to suppress the Vul phenotype of *lin-24(n2050)* using germ-line transformation. This experiment was performed essentially as previously described (Mello *et al.* 1991) with the plasmid pRF4 (80 μg/ml) as the co-injection marker. To clone *lin-33* we amplified DNA from the 156-kb region between a polymorphism at position 5412 of cosmid C10G6 and *unc-44* from *lin-33(n1302)* animals using the Expand Long Template PCR System (Roche Applied Science, Indianapolis, IN) according to the manufacturer's instructions. This amplified DNA was then injected into *unc-76(e911)* animals, using the plasmid P76-16B (Bloom and Horvitz 1997) (50 μg/ml) as a co-injection marker, to identify DNA that caused the vulvaless phenotype.

Isolation of *lin-24* cDNAs: A 10.8-kb *Sma*I-*Nco*I fragment from cosmid T20H7 was used to screen >800,000 plaques of a λ-ZAP cDNA library derived from mixed-stage poly(A)-positive RNA collection as previously described (Barstead and Waterston 1989). Fourteen plaques were isolated, 6 of which hybridized to fragments of the 10.8-kb fragment sufficient to rescue the vulvaless phenotype of *lin-24(n2050)* animals.

Determination of mutant allele sequences: We used PCR-amplified regions of genomic DNA to determine DNA sequences. For all alleles of *lin-24* and *lin-33*, we determined the sequences of all exons and splice junctions. Sequences were determined using an AB1 373A Cycle Sequencer or ABI Prism 3100 Genetic Analyzer (Applied Biosystems, Foster City, CA).

Isolation of deletion alleles: Genomic DNA pools from EMS-mutagenized animals were screened for deletions using PCR as previously described (Jansen *et al.* 1997; Liu *et al.* 1999). Deletion mutants were recovered from frozen stocks and backcrossed to the wild type six times. *lin-24(n4294Δ)* removes nucleotides 2259–3253 of cosmid B0001 (GenBank accession no. Z69634). *lin-33(n4514Δ)* removes nucleotides 28,902–29,937 of fosmid H32C10 (GenBank accession no. AF125443). *lntl-1(n4763Δ)* removes nucleotides 27,211–28,463 of cosmid C31H1 (GenBank accession no. U42848).

RESULTS

Mutations in *lin-24* and *lin-33* cause the P*n*.p cells to inappropriately undergo cell death and to adopt aberrant cell fates: Four *C. elegans* strains with mutations in the gene *lin-24* and five *C. elegans* strains with mutations in the gene *lin-33* were isolated mostly from screens for animals with the vulvaless phenotype and for animals unable to lay eggs (Trent *et al.* 1983; Ferguson and Horvitz 1985). Previous observations of *lin-24* and *lin-33* mutants using Nomarski DIC microscopy suggested that the P*n*.p cells (the posterior daughters of the 12 P cells P1–P12), some of which divide to generate descendants that form the vulva (Sulston and Horvitz 1977), frequently either die or fail to divide appropriately to form the vulva (Ferguson and Horvitz 1985; Ferguson *et al.* 1987). We confirmed and extended these observations. We observed that, in *lin-24(n432)* and *lin-33(n1043)* mutant hermaphrodites late in the first
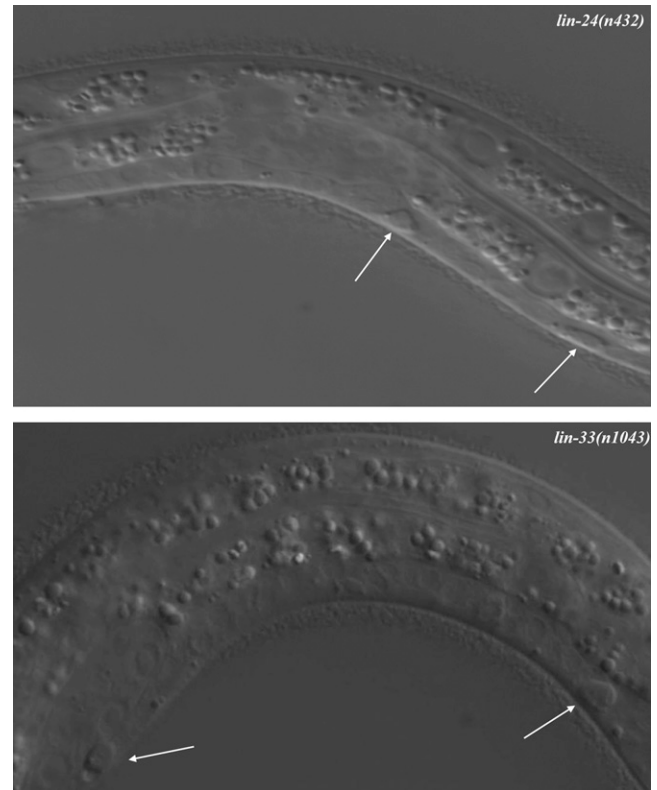

Figure 1.—The P*n*.p cells of *lin-24(n432)* and *lin-33(n1043)* mutants are morphologically abnormal. Nomarski photomicrographs of abnormal P*n*.p cells in *lin-24(n432)* and *lin-33(n1043)* L1 larvae are shown. White arrows indicate P*n*.p cells with an abnormal refractile appearance. Anterior, left; ventral, down.

larval stage (L1) or early in the second larval stage (L2), the nuclei of the P*n*.p cells increase in refractility and form noncircular often oval-shaped refractile bodies that can persist for several minutes to 3 hr (Figure 1). Once the refractility begins to decrease, within 2 hr, the nucleus becomes granular and then resolves and one of three outcomes occurs: the cell dies, the cell survives but the nucleus becomes abnormally small, or the cell survives and the nucleus regains a normal appearance. The refractile bodies seen in this process are distinct from the circular and more highly refractile corpses seen in programmed cell death (Sulston and Horvitz 1977). The refractile bodies are also distinct from the dying cells observed in *C. elegans* necrosis, in which dying cells swell to several times their original diameter (Chalfie and Sulston 1981; Chalfie and Wolinsky 1990). We observed 176 P*n*.p cells (P1–P11.p) from the mid-L1 larval stage through the early L2 larval stage in 16 *lin-24(n2050)* animals and observed that 31 died (18%), 2 survived and had small nuclei, and 143 recovered the appearance of normal P*n*.p cells (Table 1). Of the 99 P*n*.p cells we observed in 9 *lin-33(n2003)* animals, 38 (38%) died inappropriately, 6 had small nuclei, and the remaining 55 recovered the appearance of normal P*n*.p cells (Table 2). We discovered no spatial

TABLE 1

lin-24(n2050) **mutant P*n*.p cell fate at early L2 larval stage**

Animal no.	P1.p	P2.p	P3.p	P4.p	P5.p	P6.p	P7.p	P8.p	P9.p	P10.p	P11.p	No. X, sm
Wild type	+	+	+	+	+	+	+	+	+	+	+	0, 0
1	+	+	X	+	+	+	+	+	+	+	+	1, 0
2	X	+	+	+	+	+	+	+	X	+	+	2, 0
3	+	+	+	+	+	+	+	X	+	+	+	1, 0
4	+	X	+	X	+	X	+	+	X	+	+	4, 0
5	+	+	+	X	+	X	+	sm	+	+	+	2, 1
6	+	+	+	+	+	+	X	+	+	X	+	2, 0
7	+	+	+	+	X	+	+	+	+	+	+	1, 0
8	+	X	+	+	+	+	+	+	+	+	+	1, 0
9	X	+	+	+	X	+	+	+	X	+	+	3, 0
10	+	+	X	+	+	+	+	+	+	+	+	1, 0
11	+	X	X	+	X	+	+	+	+	+	+	3, 0
12	+	X	+	+	+	+	+	+	+	+	X	2, 0
13	+	+	+	+	+	X	+	+	+	+	+	1, 0
14	+	+	+	+	sm	X	+	X	+	+	+	2, 1
15	+	+	+	+	+	+	X	+	+	X	+	2, 0
16	X	+	X	+	+	+	+	+	+	+	X	3, 0
Total	3, 0	4, 0	4, 0	2, 0	3, 1	4, 0	2, 0	2, 1	3, 0	2, 0	2, 0	31, 2

lin-24(n2050) animals were observed using Nomarski optics from the mid-L1 to the early L2 larval stage. In each box, the appearance of the corresponding P*n*.p cell is noted: X, cell died; +, the nucleus looked normal; sm, the nucleus looked abnormally small. In the last column the number of P*n*.p cells that died and the number of P*n*.p cell nuclei that looked abnormally small are given, separated by a comma. In wild-type animals, all P*n*.p cells looked normal.

pattern as to which of the 11 cells examined (P1–P11.p) died. In particular, there appeared to be no preferential survival or death of the P3–P8.p cells, which have the potential to divide and differentiate to form the vulva (SULSTON and HORVITZ 1977; SULSTON *et al.* 1980; KIMBLE 1981; STERNBERG and HORVITZ 1986).

P(5–7).p normally undergo three rounds of division to generate the cells that form the vulva (SULSTON and HORVITZ 1977). Three neighboring cells P(3, 4, and 8).p, although competent to make vulval cells, normally divide once to generate two descendants that fuse with

the syncytial hypodermis (SULSTON and HORVITZ 1977; SULSTON and WHITE 1980). We examined the fates of P(3–8).p in *lin-24* and *lin-33* mutants and observed that these cells almost never divided. In *lin-24(n2050)* animals, of the 55 cells we tracked, all but 2 (96%) never divided (Table 3). Instead, these cells appeared to fuse with the hypodermal syncytium, a fate normally assumed by P(1, 2).p and P(9–12).p. Thus, *lin-24* and *lin-33* mutants are abnormal not only in P*n*.p cell survival but also in P*n*.p cell fate. The cell death of the P*n*.p cells and the failure of surviving vulval equivalence

TABLE 2

lin-33(n2003) **mutant P*n*.p cell fate at early L2 larval stage**

Animal no.	P1.p	P2.p	P3.p	P4.p	P5.p	P6.p	P7.p	P8.p	P9.p	P10.p	P11.p	No. X, sm
Wild type	+	+	+	+	+	+	+	+	+	+	+	0, 0
1	+	+	X	+	+	+	+	+	+	+	X	2, 0
2	X	+	X	+	+	+	+	X	sm	+	+	3, 1
3	+	+	+	X	X	+	X	+	+	X	+	4, 0
4	X	X	X	+	X	+	X	+	X	+	+	6, 0
5	+	X	+	sm	+	X	+	X	+	+	+	3, 1
6	+	X	X	sm	+	+	X	+	+	X	X	5, 1
7	X	sm	+	X	X	X	+	+	+	sm	sm	4, 3
8	+	X	+	X	+	+	sm	X	+	X	X	5, 1
9	X	+	X	+	+	X	X	+	X	+	X	6, 0
Total	4, 0	4, 1	5, 0	3, 2	3, 0	3, 0	4, 1	3, 0	2, 1	3, 1	4, 1	38, 7

lin-33(n2003) animals were observed using Nomarski optics from the mid-L1 to the early L2 larval stage. In each box, the appearance of the corresponding P*n*.p cell is noted: X, cell died; +, the nucleus looked normal; sm, the nucleus looked abnormally small. In the last column the number of P*n*.p cells that died and the number of P*n*.p cell nuclei that looked abnormally small are given, separated by a comma. In wild-type animals, all P*n*.p cells looked normal.

TABLE 3

**Fate of the P*n*.p cells of the vulval equivalence group
in *lin-24(n2050)* mutants**

Animal no.	P3.p	P4.p	P5.p	P6.p	P7.p	P8.p
Wild type	3°	3°	2°	1°	2°	3°
1	S	X	S	S	S	S
2	S	S	S	X	S[a]	S
3	S	S	S	S	S	S
4	S	S	S	S	S	S
5	S	S	S	X	S	S
6	S	S	S	S	S	X
7	S	S	S	1°	X	S
8	X	S	X	X	S	S
9	S	3°	X	S	X	S
10	S	S	S	S	S	S
11	S	S	S	S	X	S

lin-24(n2050) animals were picked in the early L3 larval stage and observed to the L3 molt. The fate of each cell is recorded: X, the P*n*.p cell was not present and presumed dead; S, cell persisted into the L4 larval stage without dividing and probably joined the hypodermal syncytium; 3°, tertiary fate; 2°, secondary fate; 1°, primary fate (STERNBERG and HORVITZ 1986). The top row shows the normal fates of each of the P(3–8).p cells in wild-type hermaphrodites.

[a] Nucleus was abnormally small.

group cells (P3–8.p) to divide in *lin-24* and *lin-33* mutant animals account for the vulvaless phenotype observed in these strains.

We refer to the P*n*.p cell deaths of *lin-24* and *lin-33* mutants as cytotoxic cell deaths to distinguish them from the previously studied programmed and necrotic cell deaths that are morphologically and genetically distinct (see below).

The cytotoxic cell deaths of *lin-24* and *lin-33* mutants are ultrastructurally distinct from programmed and necrotic cell deaths: We used electron microscopy to examine the ultrastructure of the P*n*.p cells of *lin-24* and *lin-33* mutants. Chromatin condensation and a shrinking of cell volume, which are hallmarks of apoptotic programmed cell death (ROBERTSON and THOMSON 1982), were not observed. Additionally, the nuclear crenellation and accumulation of single membrane-bound vacuoles observed in the nonapoptotic linker cell death were absent (ABRAHAM *et al.* 2007). Finally, we did not observe the large vacuoles characteristic of the necrotic cell deaths induced by *mec-4(gf)* and *deg-1(gf)* mutations (HALL *et al.* 1997). We noted four ultrastructural abnormalities of the refractile P*n*.p cells in *lin-24(n423)* animals, *lin-33(n1043)* animals, and *lin-33(n1043) lin-24(n432)* double-mutant animals: (1) few intact cristae and a nonelectron dense matrix in the mitochondria, (2) electron-dense puncta in the nuclei, (3) dilation of the lumen of the nuclear envelope, and (4) electron-dense membranous whorls in the cytoplasm (Figure 2 and supplemental Figure 2). Both the electron-dense membranous whorls and mitochondrial distortion are
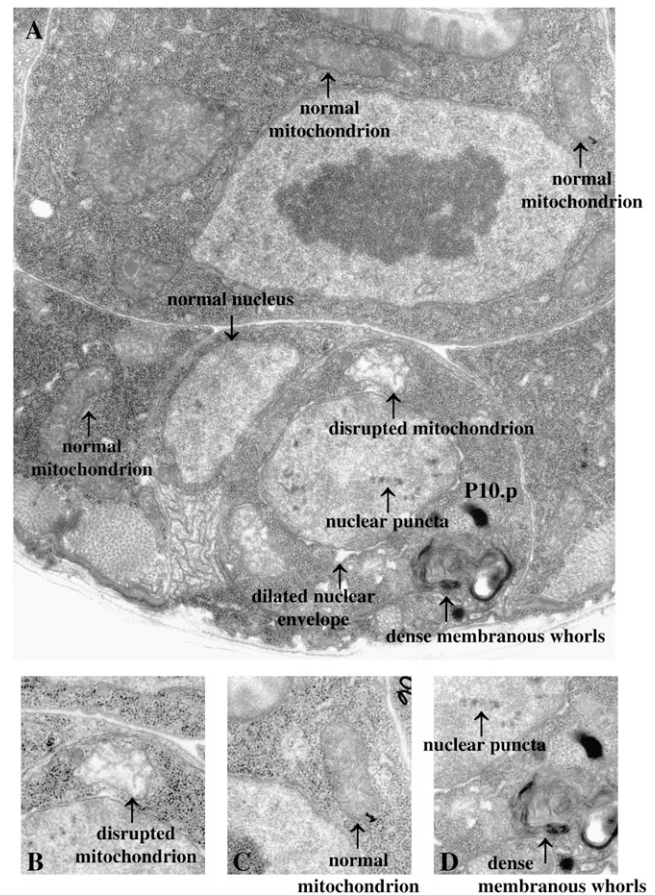

FIGURE 2.—Ultrastructural characteristics of the abnormal P*n*.p cells of *lin-24(n432)* and *lin-33(n1043)* mutants. (A) Electron micrograph of a refractile P10.p cell in a *lin-33(n1043)* mutant. Four ultrastructural characteristics of the abnormal P*n*.p cells observed in *lin-24(n432)* and *lin-33(n1043)* animals are indicated: dilated mitochondrion with disrupted internal architecture, electron-dense puncta in the nucleus, dilation of the lumen of the nuclear envelope, and dense membranous whorls. Note that these four abnormal characteristics are not observed in the adjacent cells, which all have normal cellular architecture. For comparison, a normal nucleus and normal mitochondria in neighboring cells are indicated. (B) Increased magnification of A showing a disrupted mitochondrion. (C) Increased magnification of A showing a mitochondrion with normal architecture. (D) Increased magnification of A showing the electron-dense nuclear puncta and membranous whorls.

observed in deaths induced by *mec-4(gf)* and *deg-1(gf)* mutations (HALL *et al.* 1997). Nonetheless, together the four features observed in *lin-24(n432)* and *lin-33 (n1043)* mutants distinguish their abnormal cells from the dying cells observed both in programmed cell death and in the necrotic death associated with gain-of-function mutations in the genes *mec-4* and *deg-1*. Although the *lin-24-* and *lin-33*-induced cytotoxicity is distinct from the *mec-4-* and *deg-1*-induced necrotic deaths, the dilation of the nuclear envelope we observed is also observed in some mammalian necrotic deaths (WYLLIE 1981).

TABLE 4

Penetrances of cytotoxic alleles of *lin-24* and *lin-33*

Genotype	% Vul (*n*)
Wild type	0 (89)
lin-24(n432)	92 (90)
lin-24(n432)/lin-24(+)	66 (109)
lin-24(n1821)	75 (89)
lin-24(n1821)/lin-24(+)	0 (72)
lin-24(n2050)	91 (87)
lin-24(n2050)/lin-24(+)	0 (71)
lin-24(n1057)	2 (90)
lin-24(n1057)/lin-24(+)	41 (74)
lin-33(n1043)	97 (90)
lin-33(n1043)/lin-33(+)	77 (121)
lin-33(n1044)	96 (90)
lin-33(n1110)	92 (88)
lin-33(n1302)	100 (90)
lin-33(n2003)	99 (90)
lin-33(n1043) lin-24(n432)	97 (89)
lin-33(n1043) lin-24(n432)/ lin-24(+) lin-33(+)	100 (49)

The penetrance of the Vul phenotype (%) was determined as described in MATERIALS AND METHODS. All genotypes were as indicated, except for the heterozygous animals, which also were heterozygous for *unc-76(e911)*. *n*, number of animals.

The *lin-24* and *lin-33* alleles that cause cytotoxic cell death and cell-fate defects are gain-of-function mutations: To quantify the defects of different *lin-24* and *lin-33* mutants, we scored the vulvaless phenotype by determining the percentage of animals of each strain that failed to lay eggs. The penetrance of the egg-laying defect caused by eight of the nine *lin-24* and *lin-33* alleles ranged from 75 to 100% (Table 4). Some of the *lin-24* and *lin-33* alleles caused a semidominant vulvaless phenotype (Table 4). *lin-24(n1057)* was unique in that the penetrance of the vulvaless phenotype was greatest (41%; *n* = 74) when *lin-24(n1057)* was in *trans* to *lin-24(+)* but was only rarely observed in *lin-24(n1057)* homozygotes (2%; *n* = 90).

We performed gene-dosage studies using the duplication *yDp1* and counting animals that failed to properly lay eggs and as a result turned into "bags of worms." We found penetrances of this bag-of-worms phenotype as follows: *lin-24(n1057)/ lin-24(n1057)* (0% vulvaless, *n* > 300) = *lin-24(n1057)/+ / yDp1* (2% vulvaless, *n* = 153) = *lin-24(n1057)/ lin-24(n1057)/yDp1* (2% vulvaless, *n* = 141) < *lin-24(n1057)/+* (33% vulvaless, *n* > 300). (The slight difference between the percentage of animals scored as vulvaless in the bag-of-worms assay and in the egg-laying assay (see MATERIALS AND METHODS) is likely a result of the greater sensitivity of the egg-laying assay to defects in vulval development.) These data suggest that a balance between the dosages of the mutant and wild-type gene products determines the penetrance of the vulvaless phenotype, such that when the levels of the wild-type and mutant gene products are equal, the penetrance of the vulvaless phenotype is the highest. One simple interpretation is that the *lin-24* protein forms a multimer, in a *lin-24/+* heterozygote the mutant and wild-type proteins interact to form a cytotoxic complex, and having a greater dosage of either gene product results in a reduced level of the cytotoxic heteromeric protein complex.

The semidominance of some *lin-24* and *lin-33* alleles suggested that these alleles might not be loss-of-function mutations. To define the loss-of-function phenotype of these genes we sought to isolate mutations that reduce or eliminate *lin-24* and *lin-33* function. Quantification of the penetrances of the bag-of-worms phenotype of *lin-24* alleles (*n432*, *n1057*, *n1821*, and *n2050*) or *lin-33* alleles (*n1043*, *n1044*, *n1110*, *n1302*, or *n2003*) when in *trans* to the deficiencies *sDf21* and *nDf41*, respectively, which remove either *lin-24* or *lin-33*, suggested that *lin-24(n432)/ lin-24(null)* and *lin-33(n1043)/ lin-33(null)* animals were wild-type because no bag of worms were observed (supplemental Table 1). Thus, we predicted that we should be able to isolate *lin-24* and *lin-33* loss-of-function mutations as *cis*-dominant suppressors of the vulvaless phenotype of *lin-24(n432)* or *lin-33(n1043)* mutants in F$_1$ reversion screens. In two separate screens (see MATERIALS AND METHODS), we mutagenized strains that were homozygous for either *lin-24(n432)* or *lin-33(n1043)* and isolated non-Vul animals from the F$_1$ self-progeny. One isolate from each of these two screens was a good candidate to be an intragenic suppressor mutation, on the basis of its map position, which in each case was <0.09 MU from the respective mutation [*lin-24(n432 n1503)* and *lin-33(n1043 n1502)*] (data not shown). Animals homozygous for either of the intragenic revertant alleles appeared wild type, suggesting that the loss-of-function phenotype of these genes is not vulvaless and that the previously isolated alleles of *lin-24* and *lin-33* that cause the vulvaless phenotype are gain-of-function alleles. We confirmed this hypothesis once we molecularly identified *lin-24* and *lin-33* and isolated deletion alleles of these genes (see below).

The alleles of *lin-24* that cause a vulvaless phenotype fall into three categories: those that semidominantly cause a vulvaless phenotype (*n432*), those that recessively cause a vulvaless phenotype (*n1821* and *n2050*), and those that cause a vulvaless phenotype only when in *trans* to a wild-type allele (*n1057*) (Table 4). Unlike the alleles of *lin-33* that all cause a similar semidominant vulvaless phenotype, the differing natures of the *lin-24* alleles suggest that the function of *lin-24* can be altered in a variety of ways to be cytotoxic and cause the vulvaless phenotype.

Molecular identification of *lin-24* and *lin-33*: *lin-24* had been previously mapped between *unc-22* and *dpy-26* on linkage group IV (FERGUSON and HORVITZ 1985). We further mapped *lin-24* to an interval of ~300 kb located to the left of an RFLP on cosmid C41D9 present in the *C. elegans* strain N62 (G. GARRIGA, personal communication) (Figure 3A). We cloned *lin-24* using transformation
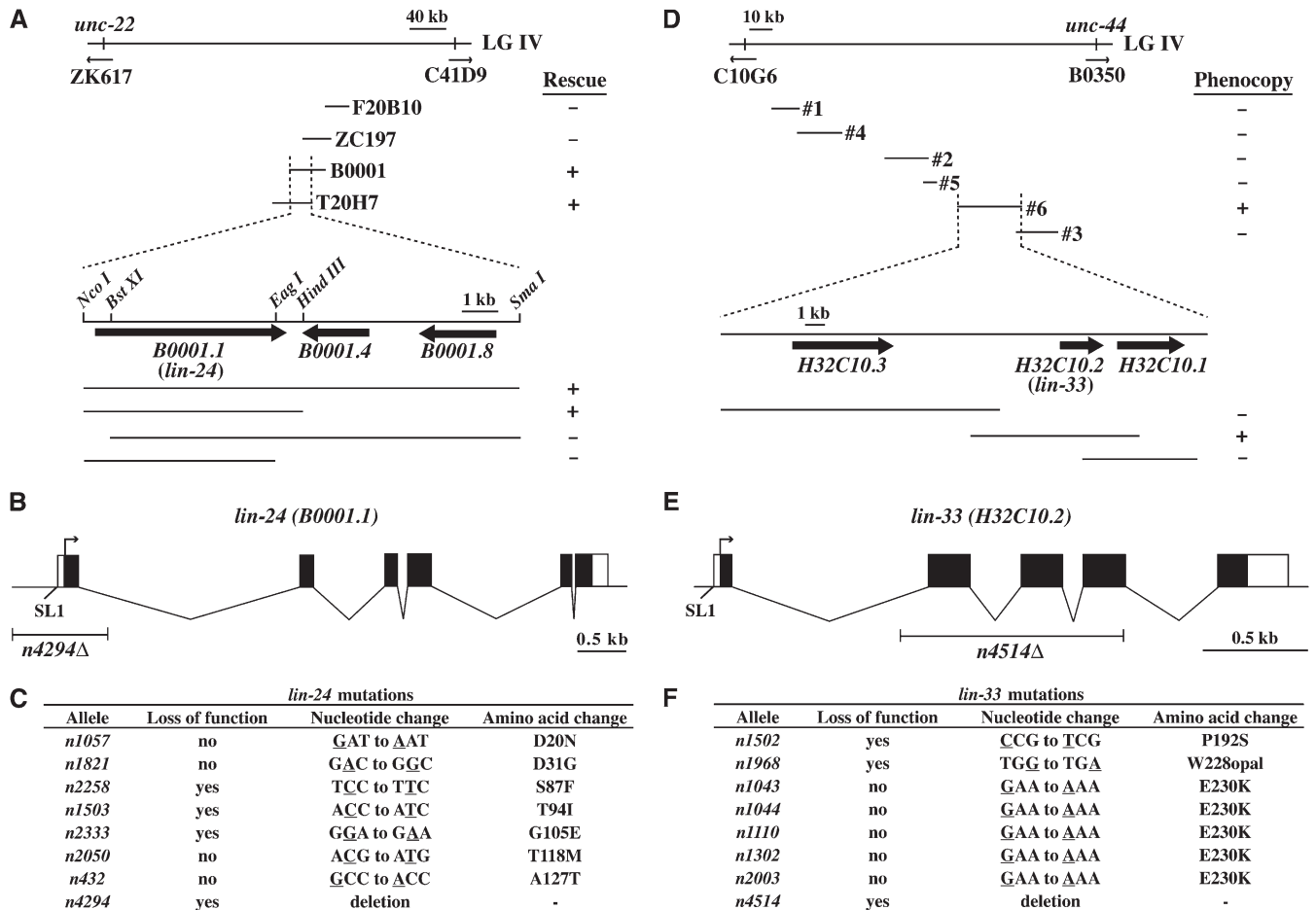
FIGURE 3.—Molecular identification of *lin-24* and *lin-33*. (A) Genetic and physical maps of the *lin-24* region. *lin-24* was mapped to the ~300-kb interval between *unc-22* and an RFLP on C41D9. The four cosmids shown were tested for their abilities to rescue the recessive vulvaless phenotype of *lin-24* mutants. The overlapping cosmids B0001 and T20H7 and an *Nco*I-*Hind*III fragment containing the gene *B0001.1* could rescue the Vulvaless phenotype. (B) The structure of the *lin-24* gene as deduced from genomic and cDNA sequences. Exons (solid boxes), 5′ and 3′ untranslated regions (open boxes), the predicted transcriptional start, and the SL1 splice leader sequence are indicated. The location of the deletion *lin-24(n4294Δ)* and the scale are indicated by the labeled horizontal lines. (C) Sequences of *lin-24* mutations. Mutated bases are underlined. Alleles were designated loss-of-function if they suppressed the semidominant vulvaless phenotype of *lin-24(n432)*. (D) Genetic and physical maps of the *lin-33* region. *lin-33* was mapped to the ~156-kb interval between a polymorphism on C10G6 and *unc-44*. PCR products generated from *lin-33(n1302)* genomic DNA spanning almost all of the shown interval were injected into *lin-33(+)* animals and tested for the ability to phenocopy the semidominant vulvaless phenotype of the *lin-33(n1302)* animals. The 26-kb PCR product no. 6 and a 9-kb PCR product containing only the gene *H32C10.2* generated a vulvaless phenotype. (E) The structure of the *lin-33* gene as deduced from genomic and cDNA sequences. Exons (solid boxes), 5′ and 3′ untranslated regions (open boxes), the predicted transcriptional start, and the SL1 splice leader sequence are indicated. The location of the deletion *lin-33(n4514Δ)* and the scale are indicated by the labeled horizontal lines. (F) Sequences of *lin-33* mutations. Mutated bases are underlined. Alleles were designated loss-of-function if they suppressed the semidominant vulvaless phenotype of *lin-33(n1043)*.

rescue by injecting wild-type cosmid DNA into *lin-24(n1821)* mutant animals, which displayed a recessive vulvaless phenotype. Of the four cosmids that we tested corresponding to sequences within the defined interval between *unc-22* and the RFLP on C41D9, two overlapping cosmids (T20H7 and B0001) rescued the recessive vulvaless phenotype of *lin-24(n1821)* animals in germ-line transformation experiments. A transgene carrying a 6.3-kb DNA sequence present in both T20H7 and B0001 and containing the single predicted gene *B0001.1* was sufficient to rescue the recessive vulvaless phenotype of *lin-24(n2050)* animals. We determined the DNA sequences of

the presumptive *lin-24* gene in each of the four different *lin-24* mutants and found that each mutant carried a different missense mutation in *B0001.1* (Figure 3C). Additionally, as predicted, we found a second mutation in *B0001.1* in *lin-24(n432 n1503)*, which was isolated in the *lin-24(n432)* reversion screen (Figure 3C). On the basis of these mapping, rescue, and sequence results, we concluded that *B0001.1* is *lin-24*. Six *lin-24* cDNAs were isolated from a mixed-stage cDNA library; the longest appeared to be full length, as it contained an SL1 *trans*-spliced leader sequence. Using this cDNA, we established the gene structure of *lin-24* shown in Figure 3B.
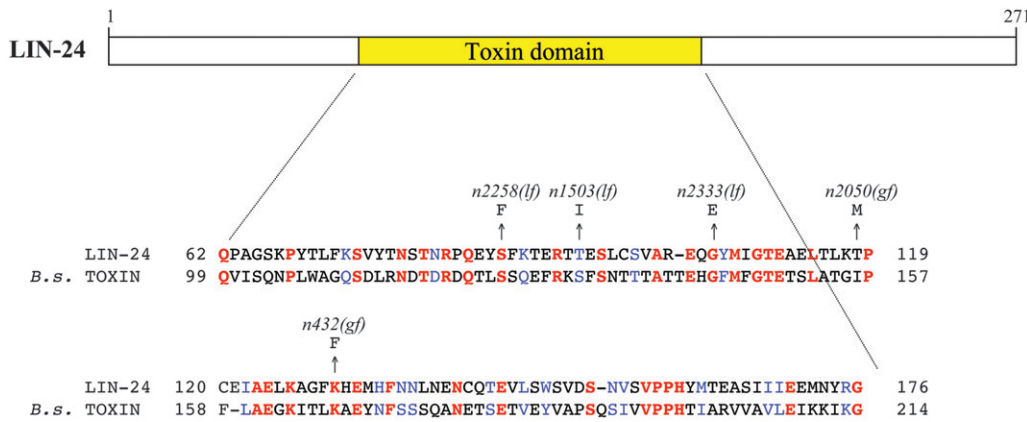
FIGURE 4.—LIN-24 contains a domain similar to that in bacterial toxins. Sequence alignment of amino acids 62–176 of LIN-24 and the Mtx3 toxin domain of the 35.8-kDa mosquitocidal toxin from *B. sphaericus* (GenBank accession no. AAB36654). Numbers at the right and left indicate amino acid positions within the respective proteins. Identical residues are colored red, and similar residues are colored blue (29% identity and 45% similarity). Missense mutations found in *lin-24* within the region of homology are indicated.

lin-33 was previously mapped between *dpy-13* and *unc-8* on linkage group IV (FERGUSON and HORVITZ 1985). We further mapped *lin-33* to an interval located to the left of *unc-44* and to the right of a polymorphism at position 5412 of cosmid C10G6 found in the *C. elegans* strain CB4856 (Figure 3D). We cloned *lin-33* by injecting DNA amplified using PCR from *lin-33(n1302)* mutant animals [which display the *lin-33(gf)* semidominant vulvaless phenotype] into *lin-33(+)* animals and determining the minimal fragment of DNA sufficient to cause a vulvaless phenotype. Seven PCR products that had been amplified from *lin-33(n1302)* genomic DNA and that together almost completely covered the 156-kb interval were tested for their abilities to phenocopy the vulvaless phenotype of *lin-33(n1302)* animals as transgenes in a *lin-33(+)* background. One of the seven PCR products, predicted to contain three genes, caused a vulvaless phenotype in wild-type animals. A single 9-kb PCR product predicted to contain one of these three genes, *H32C10.2*, also caused a vulvaless phenotype when injected into *lin-33(+)* animals. We determined the DNA sequence of *H32C10.2* from each of the five semidominant *lin-33* mutants that cause P*n*.p cell death and found that all five contain the identical missense mutation, predicted to change glutamic acid 230 to lysine (Figure 3F). Additionally, as predicted, we found a second mutation in *H32C10.2* in *lin-33(n1043 n1502)*, which was isolated in the *lin-33(n1043)* reversion screen (Figure 3F). On the basis of these mapping, rescue, and sequence results, we concluded that *H32C10.2* is *lin-33*. Two *lin-33* cDNAs have been isolated by Yuji Kohara and co-workers (Y. KOHARA, personal communication). One, yk1122h12, appears to be full length, as it contains an SL1 *trans*-spliced leader sequence. The gene structure of *lin-33* based on this cDNA is shown in Figure 3E.

LIN-24 contains a toxin domain, and LIN-33 is a novel protein: BLAST and related searches with the predicted LIN-33 protein sequence did not identify any

significant domains or homologies with other proteins. Similar searches using the LIN-24 protein sequence revealed that LIN-24 contains a domain found in many bacterial toxins. This domain, spanning amino acids 62–176, is most similar to the *Bacillus sphaericus* Mtx3 mosquitocidal toxin (Figure 4) (LIU *et al.* 1996). These toxins are thought to function by binding to eukaryotic cells and aggregating to form holes in the membrane, ultimately causing osmotic lysis by disrupting membrane permeability (GILBERT 2002). Five of the seven mutations in *lin-24* are located in the toxin-related domain (Figure 4), including the three loss-of-function alleles, suggesting that this domain has an important function in the observed cytotoxicity of mutant LIN-24. All of the loss-of-function alleles affect conserved residues. It is tempting to speculate that LIN-24 causes cytotoxicity by a mechanism similar to that of these bacterial toxins.

The *lin-24(n432)* mutation likely causes a novel gene activity: We identified the deletion alleles *lin-24(n4294Δ)* and *lin-33(n4514Δ)* by screening a library of mutagenized animals (see Figure 3 and MATERIALS AND METHODS). Animals homozygous for either deletion allele appeared wild type (Table 5), demonstrating that the null phenotype of these genes is not vulvaless. The *lin-24(n432)/lin-24(+)* and *lin-33(n1043)/lin-33(+)* strains have a more penetrant vulvaless phenotype (66 and 77% vulvaless, respectively) than *lin-24(n432)/lin-24(Δ)* and *lin-33(n1043)/lin-33(Δ)* strains (3 and 21% vulvaless, respectively), suggesting that the presence of a wild-type copy of the respective gene can increase the cytotoxicity of these alleles (Table 5). Using a duplication carrying a wild-type copy of the *lin-24* locus, we scored the penetrance of the vulvaless phenotype of strains containing different combinations of *lin-24* alleles. The relative penetrances of the vulvaless phenotype of the following *lin-24(n432)*-containing strains was *lin-24(n432)/lin-24(+)/lin-24(+)* (38% vulvaless) < *lin-24(n432)/lin-24(+)* (66%

Genotype	% Vul (*n*)
Wild type[a]	0 (89)
lin-24(n432)/ lin-24(n432)[a]	92 (90)
lin-24(n4294Δ)/ lin-24(n4294Δ)	0 (102)
lin-24(n432)/ lin-24(n4294Δ)[b]	3 (89)
lin-24(n432)/ lin-24(+)[a]	66 (109)
lin-24(n432)/ lin-24(+)/ lin-24(+)[c]	38 (56)
lin-24(n432)/ lin-24(n432)/ lin-24(+)[d]	81 (117)
lin-33(n1043)/ lin-33(n1043)[a]	97 (90)
lin-33(n4514Δ)/ lin-33(n4514Δ)	0 (72)
lin-33(n1043)/ lin-33(n4514Δ)[e]	21 (77)
lin-33(n1043)/ lin-33(+)[a]	77 (121)
lin-33(n1043) lin-24(n432)[a]	97 (89)
lin-33(n1043) lin-24(n4294Δ)	0 (56)
lin-33(n4514Δ) lin-24(n432)	0 (60)
lin-33(+) lin-24(n432)/ lin-33(n4514Δ) lin-24(+)[f]	0 (29)
lin-33(n1043) lin-24(+)/ lin-33(+) lin-24(n4294Δ)[g]	0 (12)

The number of Vul animals was determined as described in
MATERIALS AND METHODS. *n*, number of animals.

[a] These data are from Table 1.

[b] *lin-24(n432)* homozygous males were mated with *lin-24(n4294Δ) dpy-4(e1166)* hermaphrodites, and non-Dpy cross progeny were scored.

[c] This strain was of genotype *unc-30(e191) dpy-4(e1166)/lin-24(n432) dpy-4(e1166); yDp1.* Only non-Unc non-Dpy animals that segregated Unc Dpy and Unc Lin animals were scored.

[d] This strain was of genotype *lin-24(n432) dpy-4(e1166); yDp1.* Only non-Dpy animals were scored.

[e] *lin-33(n1043)* homozygous males were mated with *lin-33(n4514Δ) unc-30(e191)* hermaphrodites, and non-Unc cross progeny were scored.

[f] *lin-24(n432)* homozygous males were mated with *lin-33(n4514Δ) unc-30(e191)* hermaphrodites, and non-Unc cross progeny were scored.

[g] *lin-33(n1043)* homozygous males were mated with *lin-24(n4294Δ) dpy-4(e1166)* hermaphrodites, and non-Dpy cross progeny were scored.

vulvaless) < *lin-24(n432)/ lin-24(n432)/ lin-24(+)* (81% vulvaless) < *lin-24(n432)/ lin-24(n432)* (92% vulvaless) (Table 5), such that 0(null)/0 < m(mutant)/0 < m/+/+ < m/+ < m/m/+ < m/m. These results demonstrate that an increase in the dosage of the *lin-24(+)* gene product results in a decrease in the percentage of hermaphrodites that are vulvaless. These data indicate that the wild-type *lin-24* gene product antagonizes the cytotoxicity of the semidominant mutation. Therefore, the *lin-24(n432)* mutation does not result in an increase in the wild-type function of the gene product, function as a dominant negative, or cause a loss of function. Instead, the *lin-24(n432)* mutation probably causes the generation of an abnormal cytotoxic gene product. Technical difficulties prevented similar investigations using the free duplication *mDp4* of the effect of *n1043* on *lin-33* function (see MATERIALS AND METHODS). The relative penetrances of the vulvaless phenotype of the following

lin-33(n1043)-containing strains were *lin-33(n1043)/ lin-33(Δ)* (21% vulvaless) < *lin-33(n1043)/ lin-33(+)* (77% vulvaless) < *lin-33(n1043)/ lin-33(n1043)* (97% vulvaless) (Table 5), such that 0/0 < m/0 < m/+ < m/m. These data suggest the semidominant *n1043* mutation might cause either an increase in wild-type function or, like *lin-24(n432)*, cause a novel abnormal function.

Both *lin-24(n432)* and *lin-33(n1043)* show strikingly sharp gene-dosage effects. We suggest that the cytotoxic effects of both *lin-24(n432)* and *lin-33(n1043)* are highly sensitive to the level of mutant protein. For both mutants, the phenotype of *lin/+* is intermediate between that of *lin/*deletion and *lin/lin*. This result indicates that the level of gene expression is critical for the mutant gene products to be cytotoxic.

We also isolated a deletion allele of a gene that encodes the only protein that is highly similar to LIN-24 (32% identical and 51% similar), *lntl-1* [**lin**-24 (**t**wenty-four) **l**ike]. Both the *lntl-1(n4763Δ)* single mutant and the *lntl-1(n4763Δ) lin-24(n4294Δ)* double mutant appeared wild type. The wild-type phenotype of the doubly mutant strain *lntl-1(n4763Δ) lin-24(n4294Δ)* suggests that these two genes do not function redundantly in a critical process in *C. elegans*. There are no *C. elegans* genes that encode proteins with similarity to LIN-33.

The cytotoxic effect of *lin-24* and *lin-33* each requires the function of the other gene: In addition to isolating loss-of-function alleles of both *lin-24* and *lin-33* in their respective dominant suppressor screens, we also isolated alleles of the other gene. Specifically, we obtained one loss-of-function allele of *lin-33*, *n1968*, in the *lin-24(n432)* screen and one loss-of-function allele of *lin-24*, *n2333*, in the *lin-33(n1043)* screen. These results suggested a genetic interaction between *lin-24* and *lin-33*, which we explored further using our deletion alleles. Strains of the genotypes *lin-33(n1043) lin-24(n4294Δ)* or *lin-33(n4514Δ) lin-24(n432)* were phenotypically wild type (Table 5). Additionally, as suggested by their isolation in F[1] screens, loss-of-function alleles of *lin-24* and *lin-33* can each suppress the vulvaless phenotype caused by gain-of-function mutations in the other gene when the former are present only in one copy (data not shown). For example, animals of the genotype *lin-33(n1043) lin-24(n4294Δ)/ lin-33(n1043) lin-24(+)* were not vulvaless, so a loss of one copy of *lin-24* was able to suppress the vulvaless phenotype of *lin-33(gf)* mutant animals. Similarly, the vulvaless phenotype of *lin-24(n432)/ lin-24(+)* animals was completely suppressed by the loss of one copy of *lin-33*, and the vulvaless phenotype of *lin-33(n1043)/ lin-33(+)* animals was completely suppressed by the loss of one copy of *lin-24* (Table 5). Together these results demonstrate that the cytotoxic forms of *lin-24* and *lin-33* each require the function of the other gene for their cytotoxicities.

***lin-24*- and *lin-33*-induced cytotoxicity is partially dependent on the genes that function to engulf and degrade dying cells:** To determine whether genes in-
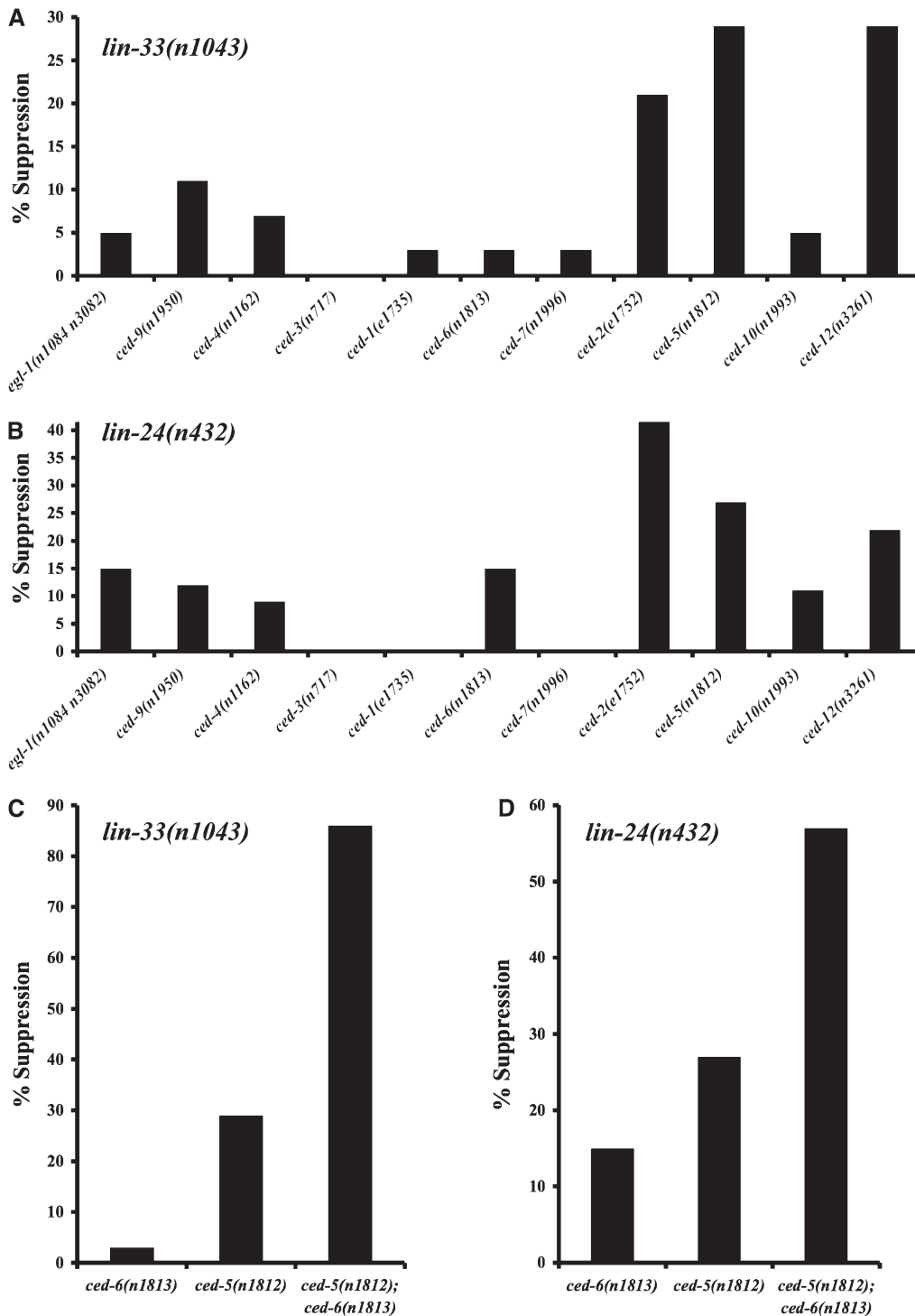
FIGURE 5.—The cytotoxicity of *lin-24(n432)* and *lin-33(n1043)* is partially dependent on genes that mediate the removal of apoptotic cell corpses. The penetrances of the vulvaless phenotypes of *lin-24(n432)*; *ced* and *lin-33(n1043)*; *ced* strains were analyzed and the percentage of suppression was calculated as described (see MATERIALS AND METHODS). At least 56 animals were assayed for each genotype. (A) Mutations in some of the genes that act in programmed cell death partially suppress the vulvaless phenotype of *lin-33(n1043)* animals. Genes are organized in the following order along the x-axis: cell-killing genes in order of action (*egl-1*, *ced-9*, *ced-4*, and *ced-3*); one of two partially redundant engulfment pathways (*ced-1*, *ced-6*, and *ced-7*); and the other partially redundant engulfment pathway (*ced-2*, *ced-5*, *ced-10*, and *ced-12*). (B) Mutations in some of the genes required for programmed cell death partially suppress the vulvaless phenotype of *lin-24(n432)* animals. (C) A *ced-5* and *ced-6* double mutant was more strongly suppressed for the vulvaless phenotype caused by *lin-33(n1043)* than was either single mutant. (D) A *ced-5* and *ced-6* double mutant was more strongly suppressed for the vulvaless phenotype caused by *lin-24(n432)* than was either single mutant.

volved in programmed cell deaths in *C. elegans* are also involved in the *lin-24-* or *lin-33-*induced cytotoxicity, we tested mutations in these genes for effects on the vulvaless phenotype of *lin-24(n432)* and *lin-33(1043)* animals. Loss-of-function mutations of genes that promote programmed cell death and a protective gain-of-function allele of *ced-9* had a modest effect on the vulvaless phenotype (Figure 5, A and B). Notably, elim-

ination of the caspase gene *ced-3*, the most downstream gene that functions in the killing step of all programmed cell deaths, had no effect on the vulvaless phenotype of *lin-24(n432)* and *lin-33(n1043)* animals. Loss-of-function alleles of the cell-death genes *ced-2*, *ced-5*, and *ced-12* most strongly suppressed the vulvaless phenotype of *lin-24(n432)* and *lin-33(n1043)* animals (Figure 5, A and B). *ced-2*, *ced-5*, and *ced-12* function together in one of two

engulfment pathways involved in the removal of cell corpses during programmed cell death (ELLIS *et al.* 1991; GUMIENNY *et al.* 2001; WU *et al.* 2001; ZHOU *et al.* 2001). *ced-10* is also proposed to function together with *ced-2*, *ced-5*, and *ced-12* (ELLIS *et al.* 1991; GUMIENNY *et al.* 2001; WU *et al.* 2001; ZHOU *et al.* 2001). Since *ced-10* is an essential gene, we used a partial loss-of-function allele, which might explain why we did not observe suppression of the vulvaless phenotype by this allele of *ced-10*. Loss-of-function alleles of genes that function together in the second engulfment pathway, *ced-1*, *ced-6*, and *ced-7*, did not suppress the vulvaless phenotype of *lin-24(n432)* and *lin-33(n1043)* animals (Figure 5, A and B).

We also examined the ability of mutations disrupting genes that function in programmed cell death to suppress the vulvaless phenotype of animals heterozygous for *lin-24(n432)* or *lin-33(n1043)*. Since the penetrances of the vulvaless phenotype caused by these alleles are weaker when heterozygous, this background might be sensitized such that it enables detection of roles in the cytotoxicity for additional genes. As expected from the results with *lin-24(n432)* and *lin-33(n1043)* homozygotes, loss-of-function mutations in *ced-2*, *ced-5*, and *ced-12* strongly suppressed the vulvaless phenotype of animals heterozygous for the cytotoxic mutations (supplemental Figure 1). For example, *ced-12* mutations almost completely restored the ability of either *lin-24(n432)/lin-24(+)* or *lin-33(n1043)/lin-33(+)* animals to lay eggs (97% suppression for both; $n = 20$ and 50, respectively). When *lin-24(n432)* or *lin-33(n1043)* was heterozygous, alleles of additional cell-death genes were able to suppress the vulvaless phenotype. For example, the partial loss-of-function allele *ced-10(n1993)* strongly suppressed both *lin-24(n432)/lin-24(+)* and *lin-33(n1043)/lin-33(+)*, supporting the view that *ced-10* might act with *ced-2*, *ced-5*, and *ced-12* in promoting the cytotoxicity.

Unexpectedly, these experiments also revealed roles for other genes that function in programmed cell death. For example, loss of the BH3-only killer gene *egl-1*, the function of which is required for essentially all somatic programmed cell deaths in *C. elegans* (CONRADT and HORVITZ 1998), strongly suppressed the vulvaless phenotype of animals heterozygous for *lin-24(n432)* or for *lin-33(n1043)* (88 and 40%, respectively; $n = 67$ and 63, respectively). Additionally, the *lin-24(n432)/lin-24(+)* strain was suppressed by loss-of-function mutations of *ced-4*, *ced-1*, and *ced-6* (58, 50, and 77%, respectively; $n = 68$, 70, and 67, respectively). The penetrance of the vulvaless phenotype of *lin-24(n432)* mutants is less than that of *lin-33(n1043)* mutants, especially when heterozygous, and presumably for this reason is more easily modified by the loss of function of genes that act in programmed cell death.

To determine the effect of simultaneously eliminating the two partially redundant engulfment pathways on the cytotoxicity, we constructed strains mutant in both *ced-5* and *ced-6* in combination with homozygous *lin-24(n432)*

TABLE 6

***lin-33(n1043)*- and *lin-24(n432)*-induced P*n*.p cell death is partially dependent on genes that mediate the removal of apoptotic corpses**

Genotype	Average no. of P*n*.p nuclei ± SD
Wild type	11
lin-33(n1043)	6.5 ± 1.4
ced-2(e1752) lin-33(n1043)	9.0 ± 1.1
ced-6(n1813); lin-33(n1043) ced-5(n1812)	10.1 ± 0.8
lin-24(n432)	7.6 ± 1.6
ced-2(e1752) lin-24(n432)	10.6 ± 0.6
ced-6(n1813); ced-5(n1812) lin-24(n432)	9.8 ± 0.9

The average number of P*n*.p nuclei per animal was determined by counting the number of P*n*.p nuclei present ∼24 hr after hatching using Nomarski optics. Twenty animals were examined for each strain.

or *lin-33(n1043)*. The elimination of both engulfment pathways suppressed the vulvaless phenotype to a greater extent than did the elimination of either single engulfment pathway (Figure 5, C and D).

To determine if the mutations that most strongly suppressed the vulvaless phenotype of *lin-24(n432)* and *lin-33(n1043)* animals [*i.e.*, *ced-2(e1752)* and the combination of *ced-5(n1812)* and *ced-6(n1813)*] affected P*n*.p cell survival, we counted the number of P*n*.p cell nuclei present in these strains. Consistent with the observed suppression of the vulvaless phenotype, P*n*.p cell death was suppressed in each of the strains examined (Table 6). Unlike the *lin-24(n432)* and *lin-33(n1043)* strains, when P*n*.p cells were missing in the suppressed strains, a cell corpse was usually present at the location of the missing P*n*.p cell. This observation suggests that when a P*n*.p cell dies, its removal requires the genes that mediate the removal of apoptotic corpses. Consistent with this genetically established role for the process of engulfment in P*n*.p cell death, our electron microscopic studies of P*n*.p cells in *lin-24* and *lin-33* mutants indicate that dying P*n*.p cells can be engulfed by neighboring cells (supplemental Figure 2).

Together the observed suppression both of the vulvaless phenotype and of P*n*.p cell death indicates that the engulfment process, and most importantly the engulfment pathway involving *ced-2*, *ced-5*, and *ced-12*, plays an important role in promoting the cytotoxicity that affects both P*n*.p cell fate and P*n*.p cell survival caused by gain-of-function mutations in *lin-24* and *lin-33*.

DISCUSSION

Mutations in *lin-24* and *lin-33* dominantly cause the P*n*.p hypodermal blast cells, a subset of which gives rise to the vulva, to die or to fail to undergo cell division, thereby resulting in a vulvaless phenotype. We have

characterized *lin-24* and *lin-33* genetically and molecularly. We found that the mutations that result in P*n*.p cell cytotoxicity are gain-of-function mutations and that *lin-24* and *lin-33* act together to cause the abnormalities of the P*n*.p cells. Although the P*n*.p cell cytotoxicity shares some genetic and morphological characteristics with both apoptotic and necrotic cell deaths that occur in *C. elegans*, this cytotoxicity is genetically and morphologically distinct from these other cell death processes. It is also distinct from the recently described linker cell death, which is controlled by an apparently cell-autonomous program and does not involve such engulfment cell-death genes as *ced-2*, *ced-5*, and *ced-12* (ABRAHAM *et al.* 2007), which have substantial roles in *lin-24-* and *lin-33-*induced cell death. The death process caused by mutations in the uncloned gene *pvl-5*, which affects P*n*.p cells in a way that, on the basis of observations using Nomarski optics, seems similar to the effects of *lin-24* and *lin-33* mutations (JOSHI and EISENMANN 2004).

lin-24- and *lin-33-*induced cytotoxicity does not require most of the genes that act in the execution of programmed cell death, since the cytotoxicity, as measured by the suppression of the vulvaless phenotype, persists in animals homozygous for mutations in the Bcl-2 family member *ced-9*, the Apaf-1 homolog *ced-4*, and the caspase gene *ced-3*. The partial suppression of the weaker vulvaless phenotype seen in animals heterozygous for either *lin-24(n432)* or *lin-33(n1043)* by the BH3-only killer gene *egl-1* is surprising, as it suggests that *egl-1*, which is the most upstream gene that functions in all somatic programmed cell deaths (CONRADT and HORVITZ 1998), might, in cell deaths other than those occurring through the process of apoptotic programmed cell death, function independently from *ced-3*, *ced-4*, and *ced-9*. The *lin-24-* and *lin-33-*induced cytotoxicity is most strongly dependent on the functions of *ced-2*, *ced-5*, and *ced-12*, which act in one of the two partially redundant pathways that mediate the engulfment of cell corpses generated by both programmed and necrotic cell deaths (ELLIS *et al.* 1991; CHUNG *et al.* 2000; GUMIENNY *et al.* 2001; WU *et al.* 2001; ZHOU *et al.* 2001). Simultaneous elimination of the function of genes from both engulfment pathways even more strongly prevents the cytotoxicity, suggesting a more general role for engulfment that extends beyond *ced-2*, *ced-5*, and *ced-12*.

What are the molecular activities of mutant and wild-type LIN-24 and LIN-33? The toxin-like domain found in LIN-24 suggests a possible mechanism for the *lin-24-* and *lin-33-*mediated cytotoxicity. The toxins with similarity to LIN-24 are thought to form membrane complexes that alter eukaryotic membrane permeability and cause osmotic lysis (GILBERT 2002). Perhaps the *lin-24* and *lin-33* gain-of-function mutations inappropriately activate a toxin-like activity of the toxin-like domain of LIN-24, causing sickness and cell death. The results of our dosage studies, which indicate a novel,

abnormal activity for the allele *lin-24(n432)*, are consistent with such a model.

Given the similarity of LIN-24 to bacterial toxins, what might be the wild-type function of the *lin-24* gene product in *C. elegans*? Neither loss of *lin-24* function alone nor loss of *lin-24* function in combination with the loss of its only homolog *lntl-1* results in any obvious abnormal phenotype. Almost all genes similar to *lin-24* are found in bacteria, which *C. elegans* eats. These bacterial toxins are capable of killing animals, such as mosquitoes and cattle, by forming oligomers that increase membrane permeability and cause osmotic lysis and cellular destruction (DE MAAGD *et al.* 2003). Perhaps wild-type LIN-24 normally functions to interact with bacterial toxins and inactivate them, possibly by a mechanism that requires LIN-33. The ability of wild-type LIN-24 to antagonize mutant LIN-24 supports this possibility. Such an activity might enable *C. elegans* to safely consume or survive exposure to bacteria that produce these deadly toxins. Consistent with this possibility is the observation that *lin-24* is expressed in both the pharynx and intestine, the main tissues that are exposed to bacteria (HUNT-NEWBURY *et al.* 2007).

The role of engulfment in cell death: The observation that mutations in *ced-2*, *ced-5*, and *ced-12* reduce *lin-24-* and *lin-33-*induced cytotoxicity is similar to the observation that engulfment genes are involved not only in engulfing corpses generated by programmed cell death but also in promoting the death process itself (HOEPPNER *et al.* 2001; REDDIEN *et al.* 2001). The programmed cell death of at least one cell type, one of the pair of cells B.alapaav and B.arapaav in the male tail, appears to be entirely dependent on engulfment (HEDGECOCK *et al.* 1983). Additional studies of *lin-24-* and *lin-33-*induced cytotoxicity could provide valuable insight not only into how engulfment contributes to cytotoxicity but also into how engulfment contributes to cell killing in programmed cell death.

In contrast to programmed cell death and to *lin-24-* and *lin-33-*induced cytotoxicity, necrotic cell death is not dependent on the function of the engulfment genes. Specifically, engulfment genes act in the engulfment and removal of the necrotic corpses seen in animals with gain-of-function mutations in *mec-4*, *deg-3*, and *deg-1*, but mutations that eliminate the function of the engulfment genes appear to affect only the timing of the disappearance of these corpses and not cell survival (CHUNG *et al.* 2000). This difference demonstrates that although common mechanisms contribute to the removal of cell corpses generated by different cell-death processes, there are critical differences among these processes.

ced-2, *ced-5*, *ced-10*, and *ced-12* function in parallel to *ced-1*, *ced-6*, and *ced-7* in the rapid removal of corpses generated by programmed and necrotic cell death (ELLIS *et al.* 1991; CHUNG *et al.* 2000; GUMIENNY *et al.* 2001; WU *et al.* 2001; ZHOU *et al.* 2001). Whereas the
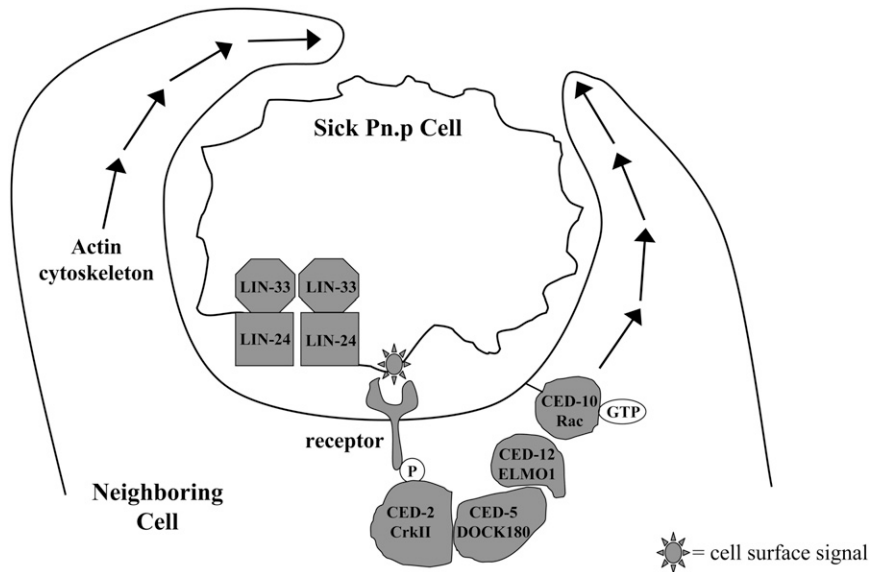
FIGURE 6.—A model for the effects of engulfment on *lin-24-* and *lin-33*-induced cytotoxicity. Gain-of-function mutations in *lin-24* and *lin-33* make the P*n*.p cells sick, possibly by forming membrane complexes that alter membrane permeability in a process that is similar to that of the bacterial toxins that share similarity with LIN-24. A consequence of this sickness is that a signal is presented on the cell membrane and recognized by a neighboring cell. The neighboring cell then promotes the cytotoxicity in a process that requires the engulfment genes *ced-2*, *ced-5*, *ced-10*, and *ced-12*, which likely act by reorganizing the actin cytoskeleton (adapted from REDDIEN and HORVITZ 2004). Additional genes that function in programmed cell death, such as *ced-6* and *egl-1*, might also play a role in *lin-24-* and *lin-33*-induced cytotoxicity.

function of the *ced-1*, *-6*, *-7* pathway is unclear, the *ced-2*, *-5*, *-10*, *-12* pathway is likely a signal transduction pathway that drives a cytoskeletal rearrangement (REDDIEN and HORVITZ 2004; MANGAHAS and ZHOU 2005). CED-2 is an *Src-homology 2* (SH2) and *Src-homology 3* (SH3) domain-containing adapter protein (REDDIEN and HORVITZ 2000), CED-10 is a Rac-like GTPase (REDDIEN and HORVITZ 2000), and CED-5 and CED-12 likely activate CED-10/Rac1 by exchanging GDP for GTP (WU and HORVITZ 1998; GUMIENNY *et al.* 2001; WU *et al.* 2001; ZHOU *et al.* 2001; BRUGNERA *et al.* 2002). The mammalian counterparts of CED-2, CED-5, and CED-12 (Crk, DOCK180, and ELMO1, respectively) regulate the CED-10 homolog Rac and function in cytoskeletal reorganization (BRUGNERA *et al.* 2002; AKAKURA *et al.* 2005; LU and RAVICHANDRAN 2006), which is important for cell migration, axonal outgrowth, and for phagocytosis in programmed cell death.

Whereas the *ced-1*, *-6*, *-7* pathway appears to be largely specific for the engulfment of cell corpses, the *ced-2*, *-5*, *-10*, *-12* pathway is involved in several other processes, including gonadal migration and axonal outgrowth (REDDIEN and HORVITZ 2004; MANGAHAS and ZHOU 2005), as well as the promotion of *lin-24-* and *lin-33*-induced cytotoxicity. We suggest that the *ced-2*, *-5*, *-10*, *-12* pathway responds to a signal presented on the surface of a cell that is sick or dying (Figure 6). It is possible that the signal presented by the cells affected by *lin-24-* and *lin-33*-induced cytotoxicity is the same as that recognized by the *ced-2*, *-5*, *-10*, *-12* pathway in programmed cell death. The *ced-1*, *-6*, *-7* pathway, by contrast, might recognize a different signal that is more specific to corpses generated by programmed cell death.

The role of the engulfment genes in promoting the cytotoxicity that affects the fate and survival of the P*n*.p cells in *lin-24* and *lin-33* mutant animals expands the

established role for engulfment in cell killing. If the promotion of death by engulfing cells is a general phenomenon for many sick, injured, or apoptotic cells, pharmacological inhibition of engulfment might broadly promote the survival of dying cells. The ability to simultaneously promote cell survival of both apoptotic and injured cells could greatly limit tissue damage in critical clinical situations, such as after traumatic brain injury or a myocardial infarction, during which cells die by both apoptotic and nonapoptotic mechanisms (KRIJNEN *et al.* 2002; MEHTA *et al.* 2007).

LITERATURE CITED

ABRAHAM, M. C., Y. LU and S. SHAHAM, 2007 A morphologically conserved nonapoptotic program promotes linker cell death in *Caenorhabditis elegans*. Dev. Cell. **12:** 73–86.

AKAKURA, S., B. KAR, S. SINGH, L. CHO, N. TIBREWAL *et al.*, 2005 C-terminal SH3 domain of CrkII regulates the assembly and function of the DOCK180/ELMO Rac-GEF. J. Cell. Physiol. **204:** 344–351.

BARGMANN, C. I., E. HARTWIEG and H. R. HORVITZ, 1993 Odorant-selective genes and neurons mediate olfaction in *C. elegans*. Cell **74:** 515–527.

BARSTEAD, R. J., and R. H. WATERSTON, 1989 The basal component of the nematode dense-body is vinculin. J. Biol. Chem. **264:** 10177–10185.

BERGER, A. J., A. C. HART and J. M. KAPLAN, 1998 G alpha$_s$-induced neurodegeneration in *Caenorhabditis elegans*. J. Neurosci. **18:** 2871–2880.

BLOOM, L., and H. R. HORVITZ, 1997 The *Caenorhabditis elegans* gene *unc-76* and its human homologs define a new gene family in-

volved in axonal outgrowth and fasciculation. Proc. Natl. Acad. Sci. USA **94:** 3414–3419.

BRENNER, S., 1974   The genetics of *Caenorhabditis elegans.* Genetics **77:** 71–94.

BRUGNERA, E., L. HANEY, C. GRIMSLEY, M. LU, S. F. WALK *et al.*, 2002   Unconventional Rac-GEF activity is mediated through the Dock180-ELMO complex. Nat. Cell Biol. **4:** 574–582.

CHALFIE, M., and J. SULSTON, 1981   Developmental genetics of the mechanosensory neurons of *Caenorhabditis elegans.* Dev. Biol. **82:** 358–370.

CHALFIE, M., and E. WOLINSKY, 1990   The identification and suppression of inherited neurodegeneration in *Caenorhabditis elegans.* Nature **345:** 410–416.

CHUNG, S., T. L. GUMIENNY, M. O. HENGARTNER and M. DRISCOLL, 2000   A common set of engulfment genes mediates removal of both apoptotic and necrotic cell corpses in *C. elegans.* Nat. Cell. Biol. **2:** 931–937.

CLARK, D. V., and D. L. BAILLIE, 1992   Genetic analysis and complementation by germ-line transformation of lethal mutations in the *unc-22* IV region of *Caenorhabditis elegans.* Mol. Gen. Genet. **232:** 97–105.

CONRADT, B., and H. R. HORVITZ, 1998   The *C. elegans* protein EGL-1 is required for programmed cell death and interacts with the Bcl-2-like protein CED-9. Cell **93:** 519–529.

DE MAAGD, R. A., A. BRAVO, C. BERRY, N. CRICKMORE and H. E. SCHNEPF, 2003   Structure, diversity, and evolution of protein toxins from spore-forming entomopathogenic bacteria. Annu. Rev. Genet. **37:** 409–433.

DEGTEREV, A., M. BOYCE and J. YUAN, 2003   A decade of caspases. Oncogene **22:** 8543–8567.

DELONG, L., L. P. CASSON and B. J. MEYER, 1987   Assessment of X chromosome dosage compensation in *Caenorhabditis elegans* by phenotypic analysis of *lin-14.* Genetics **117:** 657–670.

DRISCOLL, M., and M. CHALFIE, 1991   The *mec-4* gene is a member of a family of *Caenorhabditis elegans* genes that can mutate to induce neuronal degeneration. Nature **349:** 588–593.

DRISCOLL, M., and B. GERSTBREIN, 2003   Dying for a cause: invertebrate genetics takes on human neurodegeneration. Nat. Rev. Genet. **4:** 181–194.

EDINGER, A. L., and C. B. THOMPSON, 2004   Death by design: apoptosis, necrosis and autophagy. Curr. Opin. Cell Biol. **16:** 663–669.

ELLIS, R. E., D. M. JACOBSON and H. R. HORVITZ, 1991   Genes required for the engulfment of cell corpses during programmed cell death in *Caenorhabditis elegans.* Genetics **129:** 79–94.

FERGUSON, E. L., and H. R. HORVITZ, 1985   Identification and characterization of 22 genes that affect the vulval cell lineages of the nematode *Caenorhabditis elegans.* Genetics **110:** 17–72.

FERGUSON, E. L., P. W. STERNBERG and H. R. HORVITZ, 1987   A genetic pathway for the specification of the vulval cell lineages of *Caenorhabditis elegans.* Nature **326:** 259–267.

GILBERT, R. J., 2002   Pore-forming toxins. Cell. Mol. Life Sci. **59:** 832–844.

GUMIENNY, T. L., E. LAMBIE, E. HARTWIEG, H. R. HORVITZ and M. O. HENGARTNER, 1999   Genetic control of programmed cell death in the *Caenorhabditis elegans* hermaphrodite germline. Development **126:** 1011–1022.

GUMIENNY, T. L., E. BRUGNERA, A. C. TOSELLO-TRAMPONT, J. M. KINCHEN, L. B. HANEY *et al.*, 2001   CED-12/ELMO, a novel member of the CrkII/Dock180/Rac pathway, is required for phagocytosis and cell migration. Cell **107:** 27–41.

HALL, D. H., G. GU, J. GARCIA-ANOVEROS, L. GONG, M. CHALFIE *et al.*, 1997   Neuropathology of degenerative cell death in *Caenorhabditis elegans.* J. Neurosci. **17:** 1033–1045.

HEDGECOCK, E. M., J. E. SULSTON and J. N. THOMSON, 1983   Mutations affecting programmed cell deaths in the nematode *Caenorhabditis elegans.* Science **220:** 1277–1279.

HENGARTNER, M. O., and H. R. HORVITZ, 1994   *C. elegans* cell survival gene *ced-9* encodes a functional homolog of the mammalian proto-oncogene bcl-2. Cell **76:** 665–676.

HENGARTNER, M. O., R. E. ELLIS and H. R. HORVITZ, 1992   *Caenorhabditis elegans* gene *ced-9* protects cells from programmed cell death. Nature **356:** 494–499.

HOCKENBERY, D., G. NUNEZ, C. MILLIMAN, R. D. SCHREIBER and S. J. KORSMEYER, 1990   Bcl-2 is an inner mitochondrial membrane protein that blocks programmed cell death. Nature **348:** 334–336.

HOEPPNER, D. J., M. O. HENGARTNER and R. SCHNABEL, 2001   Engulfment genes cooperate with *ced-3* to promote cell death in *Caenorhabditis elegans.* Nature **412:** 202–206.

HORVITZ, H. R., 1999   Genetic control of programmed cell death in the nematode *Caenorhabditis elegans.* Cancer Res. **59:** 1701s–1706s.

HUNT-NEWBURY, R., R. VIVEIROS, R. JOHNSEN, A. MAH, D. ANASTAS *et al.*, 2007   High-throughput in vivo analysis of gene expression in *Caenorhabditis elegans.* PLoS Biol. **5:** e237.

JANSEN, G., E. HAZENDONK, K. L. THIJSSEN and R. H. PLASTERK, 1997   Reverse genetics by chemical mutagenesis in *Caenorhabditis elegans.* Nat. Genet. **17:** 119–121.

JOSHI, P., and D. M. EISENMANN, 2004   The *Caenorhabditis elegans pvl-5* gene protects hypodermal cells from *ced-3*-dependent, *ced-4*-independent cell death. Genetics **167:** 673–685.

KIMBLE, J., 1981   Alterations in cell lineage following laser ablation of cells in the somatic gonad of *Caenorhabditis elegans.* Dev. Biol. **87:** 286–300.

KIMBLE, J., and D. HIRSH, 1979   The postembryonic cell lineages of the hermaphrodite and male gonads in *Caenorhabditis elegans.* Dev. Biol. **70:** 396–417.

KORSWAGEN, H. C., J. H. PARK, Y. OHSHIMA and R. H. PLASTERK, 1997   An activating mutation in a *Caenorhabditis elegans* Gs protein induces neural degeneration. Genes Dev. **11:** 1493–1503.

KRIJNEN, P. A., R. NIJMEIJER, C. J. MEIJER, C. A. VISSER, C. E. HACK *et al.*, 2002   Apoptosis in myocardial ischaemia and infarction. J. Clin. Pathol. **55:** 801–811.

LAI, C. C., K. HONG, M. KINNELL, M. CHALFIE and M. DRISCOLL, 1996   Sequence and transmembrane topology of MEC-4, an ion channel subunit required for mechanotransduction in *Caenorhabditis elegans.* J. Cell Biol. **133:** 1071–1081.

LETTRE, G., and M. O. HENGARTNER, 2006   Developmental apoptosis in *C. elegans*: a complex CEDnario. Nat. Rev. Mol. Cell Biol. **7:** 97–108.

LIU, J. W., A. G. PORTER, B. Y. WEE and T. THANABALU, 1996   New gene from nine *Bacillus sphaericus* strains encoding highly conserved 35.8-kilodalton mosquitocidal toxins. Appl. Environ. Microbiol. **62:** 2174–2176.

LIU, L. X., J. M. SPOERKE, E. L. MULLIGAN, J. CHEN, B. REARDON *et al.*, 1999   High-throughput isolation of *Caenorhabditis elegans* deletion mutants. Genome Res. **9:** 859–867.

LU, M., and K. S. RAVICHANDRAN, 2006   Dock180-ELMO cooperation in Rac activation. Methods Enzymol. **406:** 388–402.

MANGAHAS, P. M., and Z. ZHOU, 2005   Clearance of apoptotic cells in *Caenorhabditis elegans.* Semin. Cell Dev. Biol. **16:** 295–306.

MEHTA, S. L., N. MANHAS and R. RAGHUBIR, 2007   Molecular targets in cerebral ischemia for developing novel therapeutics. Brain Res. Rev. **54:** 34–66.

MELLO, C. C., J. M. KRAMER, D. STINCHCOMB and V. AMBROS, 1991   Efficient gene transfer in *C. elegans:* extrachromosomal maintenance and integration of transforming sequences. EMBO J. **10:** 3959–3970.

REDDIEN, P. W., and H. R. HORVITZ, 2000   CED-2/CrkII and CED-10/Rac control phagocytosis and cell migration in *Caenorhabditis elegans.* Nat. Cell Biol. **2:** 131–136.

REDDIEN, P. W., and H. R. HORVITZ, 2004   The engulfment process of programmed cell death in *Caenorhabditis elegans.* Annu. Rev. Cell Dev. Biol. **20:** 193–221.

REDDIEN, P. W., S. CAMERON and H. R. HORVITZ, 2001   Phagocytosis promotes programmed cell death in *C. elegans.* Nature **412:** 198–202.

RIDDLE, D. L., T. BLUMENTHAL, B. I. MEYER and J. R. PRIESS, 1997   *C. elegans II.* Cold Spring Harbor Laboratory Press, Plainview, N.Y.

ROBERTSON, A. M. G., and J. N. THOMSON, 1982   Morphology of programmed cell death in the ventral nerve cord of *C. elegans* larvae. J. Embryol. Exp. Morphol. **67:** 89–100.

SHAHAM, S., and H. R. HORVITZ, 1996   Developing *Caenorhabditis elegans* neurons may contain both cell-death protective and killer activities. Genes Dev. **10:** 578–591.

STERNBERG, P. W., and H. R. HORVITZ, 1986   Pattern formation during vulval development in *C. elegans.* Cell **44:** 761–772.

SULSTON, J. E., and H. R. HORVITZ, 1977   Post-embryonic cell lineages of the nematode, *Caenorhabditis elegans.* Dev. Biol. **56:** 110–156.

SULSTON, J. E., and J. G. WHITE, 1980   Regulation and cell autonomy during postembryonic development of *Caenorhabditis elegans.* Dev. Biol. **78:** 577–597.

Sulston, J. E., D. G. Albertson and J. N. Thomson, 1980 The *Caenorhabditis elegans* male: postembryonic development of nongonadal structures. Dev. Biol. **78:** 542–576.

Sulston, J. E., E. Schierenberg, J. G. White and J. N. Thomson, 1983 The embryonic cell lineage of the nematode *Caenorhabditis elegans*. Dev. Biol. **100:** 64–119.

Syntichaki, P., K. Xu, M. Driscoll and N. Tavernarakis, 2002 Specific aspartyl and calpain proteases are required for neurodegeneration in *C. elegans*. Nature **419:** 939–944.

Treinin, M., and M. Chalfie, 1995 A mutated acetylcholine receptor subunit causes neuronal degeneration in *C. elegans*. Neuron **14:** 871–877.

Trent, C., N. Tsuing and H. R. Horvitz, 1983 Egg-laying defective mutants of the nematode *Caenorhabditis elegans*. Genetics **104:** 619–647.

Vaux, D. L., S. Cory and J. M. Adams, 1988 *Bcl-2* gene promotes haemopoietic cell survival and cooperates with c-*myc* to immortalize pre-B cells. Nature **335:** 440–442.

Vaux, D. L., I. L. Weissman and S. K. Kim, 1992 Prevention of programmed cell death in *Caenorhabditis elegans* by human *bcl-2*. Science **258:** 1955–1957.

Wicks, S. R., R. T. Yeh, W. R. Gish, R. H. Waterston and R. H. Plasterk, 2001 Rapid gene mapping in *Caenorhabditis elegans* using a high density polymorphism map. Nat. Genet. **28:** 160–164.

Williams, B. D., B. Schrank, C. Huynh, R. Shownkeen and R. H. Waterston, 1992 A genetic mapping system in *Caenorhabditis elegans* based on polymorphic sequence-tagged sites. Genetics **131:** 609–624.

Wu, Y. C., and H. R. Horvitz, 1998 *C. elegans* phagocytosis and cell-migration protein CED-5 is similar to human DOCK180. Nature **392:** 501–504.

Wu, Y. C., M. C. Tsai, L. C. Cheng, C. J. Chou and N. Y. Weng, 2001 *C. elegans* CED-12 acts in the conserved crkII/DOCK180/Rac pathway to control cell migration and cell corpse engulfment. Dev. Cell **1:** 491–502.

Wyllie, A. H., 1981 Cell death: a new classification separating apoptosis from necrosis, pp. 9–34 in *Cell Death in Biology and Pathology*, edited by I. D. Bowen and R. A. Lockshin. Chapman & Hall, London.

Xu, K., N. Tavernarakis and M. Driscoll, 2001 Necrotic cell death in *C. elegans* requires the function of calreticulin and regulators of Ca(2+) release from the endoplasmic reticulum. Neuron **31:** 957–971.

Yuan, J., S. Shaham, S. Ledoux, H. M. Ellis and H. R. Horvitz, 1993 The *C. elegans* cell death gene *ced-3* encodes a protein similar to mammalian interleukin-1 beta-converting enzyme. Cell **75:** 641–652.

Zhou, Z., E. Caron, E. Hartwieg, A. Hall and H. R. Horvitz, 2001 The *C. elegans* PH domain protein CED-12 regulates cytoskeletal reorganization via a Rho/Rac GTPase signaling pathway. Dev. Cell **1:** 477–489.

Zong, W. X., and C. B. Thompson, 2006 Necrotic death as a cell fate. Genes Dev. **20:** 1–15.